A large time step 1D upwind explicit scheme (CFL>1): application to shallow water equations

M. Morales-Hernandez, P. García-Navarro and J. Murillo

Fluid Mechanics. LIFTEC, EINA, Universidad de Zaragoza. Zaragoza, Spain

Abstract

It is possible to relax the Courant-Friedrichs-Lewy condition over the time step when using explicit schemes. This method, proposed by Leveque, provides accurate and correct solutions of non-sonic shocks. Rarefactions need some adjustments which are explored in the present work with scalar equation and systems of equations. The non-conservative terms that appear in systems of conservation laws introduce an extra difficulty in practical application. The way to deal with source terms is incorporated into the proposed procedure. The boundary treatment is analysed and a reflection wave technique is considered. In presence of strong strong discontinuities or important source terms, a strategy is proposed to control the stability of the method allowing the largest time step possible. The performance of the above scheme is evaluated to solve the homogeneous shallow water equations and the shallow water equations with source terms.

Keywords: Large time step scheme, Hyperbolic conservation laws, Source terms, Boundary conditions, Shallow water flows, CFL limit

1. Introduction

Upwind methods have proved a suitable way to discretize the shallow water equations being able to predict the water profile and discharges in hydraulic modelling [1]. The first order explicit upwind method, in particular, has gained widespread acceptance in this area because of its conceptual simplicity despite the time step size is restricted by stability reasons to fulfil the Courant-Friedrichs-Lewy (CFL) condition.

It is possible to relax the condition over the time step size when using explicit schemes. A generalization of the first order explicit upwind scheme, modified to allow large time steps, was explored by Leveque [2, 3] (Large Time Step, LTS) first in the scalar non-linear case and then adapted to systems of equations. It becomes stable for CFL values larger than 1 and provides accurate and correct solutions of shocks. Some difficulties can be met when a rarefaction is present in the solution so that adjustments are necessary. Other class of large time step explicit schemes based on TVD properties [4] have been analysed and tested mainly for the scalar equations or systems of equations without source terms. These will not be considered in the present work.

The LTS scheme is increasingly used because it is able to achieve a reduction in the computational time keeping reasonably accurate. Engineering applications related with atmospheric dynamics [5] and Euler equations [6] have been recently published. The shallow water equations, being a hyperbolic system of equations, are also a good candidate for the application of the LTS scheme and an overview of this scheme in the context of the shallow water system was presented in [7]. The source term treatment and the boundary conditions discretization are crucial to allow stability in presence large CFL values in realistic cases.

The source term discretization has been strongly discussed in the literature. The main focus consisting on maintaining the discrete balance between flux and source terms giving rise to well-balanced schemes [8, 9, 1] has given way to techniques that prevent instability and ensure conservation by a suitable flux difference redistribution [10] avoiding the necessity of reducing the time step below the CFL condition. The idea of using a stationary jump discontinuity representing the source term in the Riemann solution [11] and the corresponding augmented approximate Riemann solvers for the shallow water equations [12] can be incorporated to the LTS scheme. Moreover, in several situations, the presence of large source terms playing a leading role over the convective terms can lead to wrong solutions using the LTS because the wave celerity is not well estimated due to the reduced number of time steps done. A way of overcoming this situation is also proposed providing the Rankine-Hugoniot conditions derived from the Riemann problem analysis.

The boundary conditions dicretization is another issue of importance in a numerical model. In the context of the shallow water equations, open boundaries and closed boundaries can appear and must be analyzed. From the structure of the LTS scheme, information is transmitted not only to the immediate neighbouring cells but also to a number of other cells growing as the CFL value increases. Therefore, some information can cross the boundaries and a careful consideration is required in order to reproduce all kind of scenarios such as subcritical, supercritical and closed boundaries. A first approximation of the boundary treatment was also proposed in [7], where an accumulation technique was suggested in the case of closed boundaries. Another possibility called reflection technique is considered here.

This method is proposed to be a general tool for solving the 1D shallow water equations for open channel and river flow problems. Several problems such as wet/dry fronts, sonic points, changes in the flow regime or large discontinuities are already solved for the conventional upwind explicit scheme hence a kind of CFL limiter can be proposed in order to reduce the initial CFL number or directly recover the original scheme with CFL=1 when these situations are present.

The outline is as follows: the discretization is described first, for 1D scalar equations with and without source terms. In the non-linear case,the treatment of the rarefaction waves is explored. Then, the scheme is extended to systems of equations, in particular to solve the shallow water equations where bed slope and friction source terms are incorporated into the proposed procedure. The way of dealing with the boundaries is analyzed in the cases of systems and two possibilities are proposed: an accumulation technique and a reflection technique. They are tested in a dam break problem with solid wall conditions in the inlet and outlet boundaries. Moreover, the use of a parameter that limits the CFL number in the presence of big discontinuities or large source terms is proposed. Finally, the scheme is evaluated and tested trough several problems with analytical solutions where the bed slope and the friction terms plays a leading role.

2. Scalar equations

2.1. Linear scalar equation

Consider the linear scalar equation:

$$\frac{\partial u}{\partial t} + \frac{\partial f(u)}{\partial x} = 0 \tag{1}$$

where u is the conserved variable and $f(u)$ is a linear function, $f(u) = \lambda u$, $\lambda = constant$.

The numerical resolution of (1) by means of the first order upwind finite volume method starts by integrating (1) in a volume Ω.

$$\frac{\partial}{\partial t}\int_{\Omega} u d\Omega + \int_{\Omega} \frac{\partial}{\partial x} f(u) d\Omega = 0 \tag{2}$$

where $d\Omega$ denotes the volume boundary.

In the case of a uniform discrete mesh $\Omega = \Delta x$. A cell-centred upwind finite volume method is based on a piecewise constant approximation of the function. Therefore, u and f are uniform per cell and the first integral of (2) can be approximated at cell Ω_i by:

$$\frac{\partial}{\partial t}\int_{\Omega_i} u d\Omega = \frac{u_i^{n+1} - u_i^n}{\Delta t}\Delta x \tag{3}$$

After application of the Gauss theorem to the second integral in (2):

$$\int_{\Omega} \frac{\partial}{\partial x} f(u) d\Omega = f^*_{i+1/2} - f^*_{i-1/2} \tag{4}$$

where the numerical flux $f^*_{i+1/2}$ can be determined using an approximate solver. The numerical scheme can be formulated in a general way as:

$$u_i^{n+1} = u_i^n - \frac{\Delta t}{\Delta x}(f^*_{i+1/2} - f^*_{i-1/2}) \tag{5}$$

Following the upwind philosophy, which discriminates the sense of propagation according to the sign of the advection velocity, the quantities

$$\lambda^{\pm} = \frac{\lambda \pm |\lambda|}{2} \tag{6}$$

allow to express the numerical fluxes in (4) as:

$$f^*_{i+1/2} = f_i + \lambda^- \delta u_{i+1/2} \qquad f^*_{i-1/2} = f_i - \lambda^+ \delta u_{i-1/2} \tag{7}$$

Therefore, the cell updating in (5) can be reformulated as resulting from the sum of two signals instead of the difference of two numerical fluxes (Figure 1):

$$u_i^{n+1} = u_i^n - \frac{\Delta t}{\Delta x}(\delta f^+_{i-1/2} + \delta f^-_{i+1/2}) \tag{8}$$

This is a finite volume point of view centered at the cells which accumulates the arriving signals to update the value of the function at every cell. There is another way to consider this situation by looking where the signals

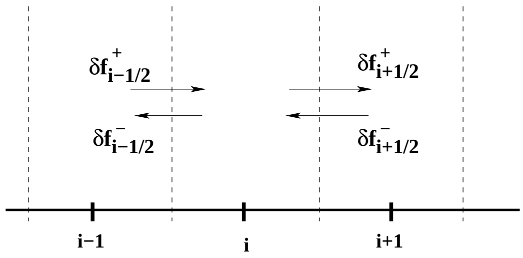

Figure 1: Contributions from left and from right in cell i

go from each interface [2]. For example, at interface $(i, i+1)$ the quantity $\nu\ \delta u_{i+1/2}$, where $\nu = \dfrac{\Delta t}{\Delta x}\lambda$ can be defined and it is sent according to the sign of λ following the algorithm:

$$\begin{aligned} &\text{if } \lambda > 0 \Rightarrow \nu\ \delta u_{i+1/2} \quad \text{updates } i+1 \\ &\text{if } \lambda < 0 \Rightarrow |\nu|\ \delta u_{i+1/2} \quad \text{updates } i \end{aligned} \tag{9}$$

Both versions of the scheme are equivalent if

$$CFL = \frac{\Delta t}{\Delta x}\lambda \leq 1 \tag{10}$$

The second approach is nevertheless preferable to extend the scheme to CFL > 1. As described by Leveque [2], the extension of the scheme to larger time steps is achieved by allowing each wave or signal to propagate independently from all others waves according to the following algorithm:

If $\lambda > 0$

$$\begin{aligned} &\delta u_{i+1/2} && \text{updates } i+1, \cdots, i+\mu_{i+1/2} \\ &(\nu - \mu)\ \delta u_{i+1/2} && \text{updates } i+\mu_{i+1/2}+1 \end{aligned} \tag{11}$$

If $\lambda < 0$

$$\begin{aligned} &\delta u_{i+1/2} && \text{updates } i, \cdots, i+\mu_{i+1/2} \\ &|\nu - \mu|\ \delta u_{i+1/2} && \text{updates } i+\mu_{i+1/2} \end{aligned} \tag{12}$$

where $\mu = int(\nu)$. Figure 2 shows how the information is sent from interface $(i, i+1)$ to the involved cells when $\lambda > 0$ (a) and when $\lambda < 0$ (b).

The proposed scheme is explicit and remains conservative. This is the basic formulation of what is called LTS scheme in this work. It is important to remark that if CFL $\leqslant$1 the scheme becomes the original first order explicit upwind scheme.

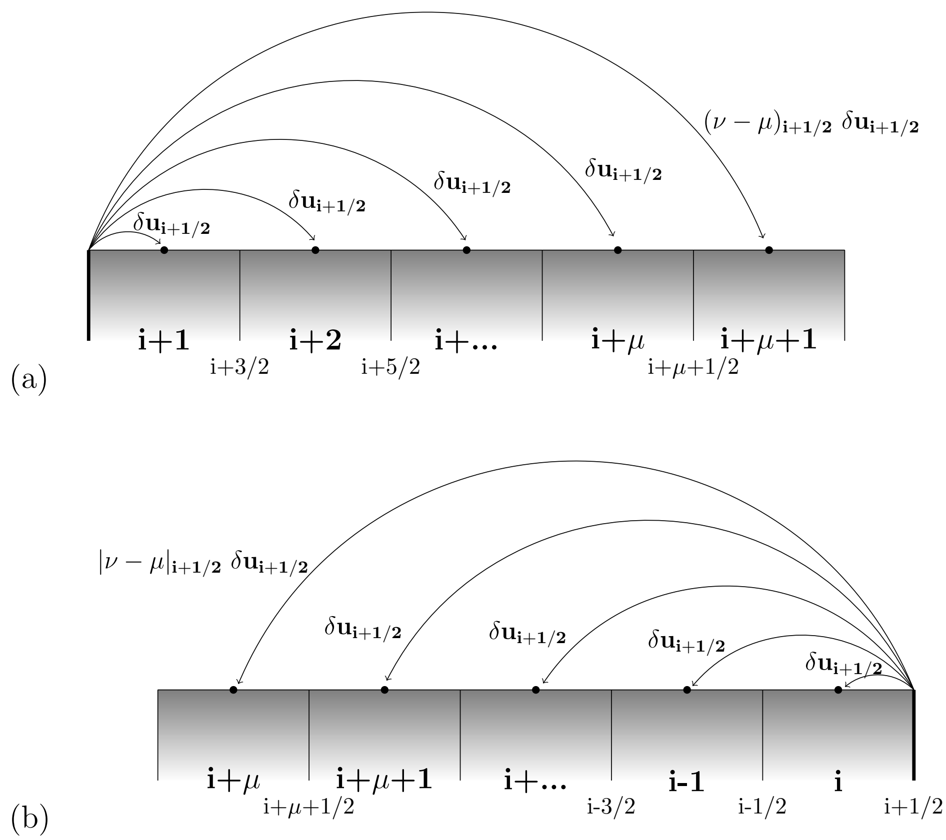

Figure 2: Scheme of the contributions from intercell *i+1/2* for $\lambda > 0$ (a) and for $\lambda < 0$ (b)

2.2. Non-linear scalar equation

Consider now the conservation law:

$$\frac{\partial u}{\partial t} + \frac{\partial f(u)}{\partial x} = 0 \tag{13}$$

where $f(u)$ is a convex non-linear function of u. So that:

$$\lambda = \frac{df}{du} \qquad \lambda = \lambda(u). \tag{14}$$

which is no longer constant. The LTS scheme, when applied to (13), requires the definition of an approximate advection celerity at the intercell as follows:

$$\widetilde{\lambda}_{i+1/2} = \frac{f(u_{i+1}) - f(u_i)}{u_{i+1} - u_i} \tag{15}$$

Certain new elements appear in this case that are going to be explored using the Burgers equation as an example.

2.2.1. Burgers equation and the Riemann Problem

The inviscid Burgers equation is a particular case of scalar conservation law of the type (13) with $f(u) = \frac{1}{2}u^2$. This equation can be written as

$$\frac{\partial u}{\partial t} + \frac{\partial}{\partial x}\left(\frac{u^2}{2}\right) = 0 \qquad \text{or} \qquad \frac{\partial u}{\partial t} + u\frac{\partial u}{\partial x} = 0 \tag{16}$$

Considering the following initial value problem or Riemann Problem (RP)

$$u(x,0) = \begin{cases} u_L & if \quad x < 0 \\ u_R & if \quad x > 0 \end{cases} \tag{17}$$

two different situations appear depending on the relative value of u_L and u_R. When $u_L > u_R$ a right moving shock develops (see Figure 3).

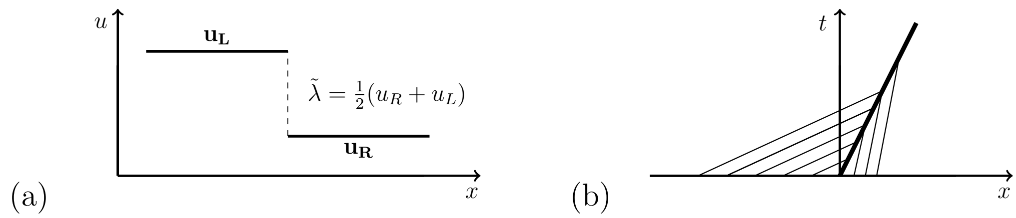

Figure 3: (a) Initial data of a shock; (b) Map of characteristic lines of a shock

The discontinuous solution of the RP in this case is

$$u(x,t) = \begin{cases} u_L & if \quad x - \tilde{\lambda}t < 0 \\ u_R & if \quad x - \tilde{\lambda}t > 0 \end{cases} \tag{18}$$

where $\tilde{\lambda}$ is the speed of the discontinuity:

$$\tilde{\lambda} = \frac{1}{2}(u_L + u_R) \tag{19}$$

Figure 4 sketches the approximate solution of the RP when dealing with a right moving shock.

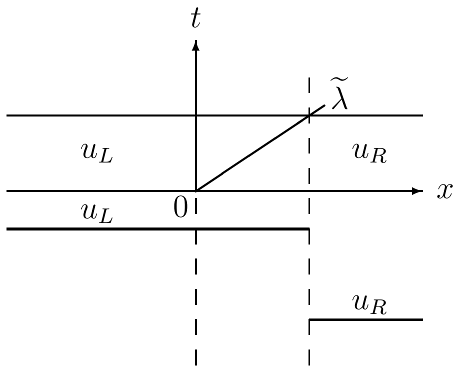

Figure 4: Discontinous solution of (17) when $u_L > u_R$

When $u_L < u_R$ (Figure 5) the solution of the RP consists of a smooth rarefaction wave connecting the two constant states u_L an u_R.

$$u(x,t) = \begin{cases} u_L & if \quad x/t \leq u_L \\ x/t & if \quad u_L < x/t < u_R \\ u_R & if \quad x/t \geq u_R \end{cases} \tag{20}$$

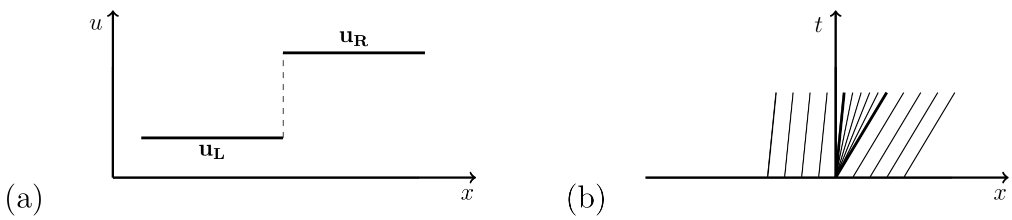

Figure 5: (a) Initial data of a rarefaction; (b) Map of characteristic lines of a rarefaction

Assuming $u_L = u_i$ and $u_R = u_{i+1}$ and integrating (13) over a suitable control volume $[-\frac{\Delta x}{2}, \frac{\Delta x}{2}] \times [0, \Delta t]$

$$\int_{\frac{-\Delta x}{2}}^{\frac{\Delta x}{2}} \hat{u}(x, \Delta t) dx = \Delta x \, (u_{i+1}^n + u_i^n) - (f(u_{i+1}^n) - f(u_i^n))\Delta t \tag{21}$$

the approximate solution of the RP $\hat{u}(x, t)$ can be derived [13].

As described in [2, 3], the LTS scheme can be used to provide an accurate and correct solution of shocks. In presence of a rarefaction, the explicit upwind scheme replaces several characteristic lines with a single line and only one intermediate state u^* is defined (see Figure 6 (a)). This approximation is effective in the conventional upwind explicit method but can fail when using CFL > 1. The proposed LTS includes several intermediate states $u_1^*, ..., u_{N_p}^*$ corresponding to several discontinuities travelling at different speeds (Figure 6(b)). The required number of discontinuities N_p is related with the strength of the RP. A good approximation could be:

$$N_p = int(\frac{\delta u \; \Delta t}{\delta x}) \tag{22}$$

where $\delta u = u_R - u_L$. The proposed way of handling rarefaction waves is always conservative.

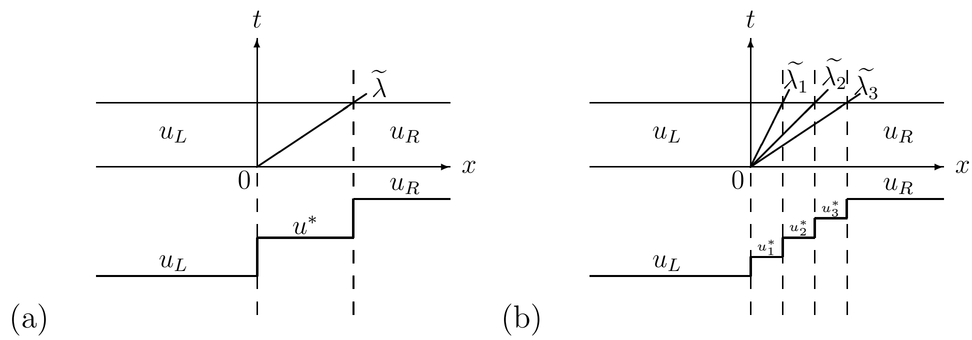

Figure 6: (a) Classical treatment of rarefaction waves in the upwind scheme; (b) Splitting treatment of rarefaction waves in the LTS scheme

In order to illustrate the performance of LTS in presence of a rarefaction, consider (16) with the initial data:

$$u(x, 0) = \begin{cases} 1.0 \quad if \quad x < 50.0 \\ 4.0 \quad if \quad x > 50.0 \end{cases} \tag{23}$$

The exact solution for this case is

$$u(x,t) = \begin{cases} 1.0 & if \quad \dfrac{x}{t} \leq 1.0 \\ \dfrac{x}{t} & if \quad 1.0 < \dfrac{x}{t} < 4.0 \\ 4.0 & if \quad \dfrac{x}{t} \geq 4.0 \end{cases} \tag{24}$$

Figure 7(a) shows the exact solution at $t = 5s$ together with the numerical results obtained with the LTS scheme on a regular mesh of $\Delta x = 1.0$. The discretization of the rarefaction in a single wave has been used and different CFL values are associated to different number of time steps (TS) as summarized in Table 1. Only in the case of CFL=1.0 an accurate solution is achieved although using 20 TS.

Figures 7(b) and 7(c) show the exact solution at $t = 5s$ and the numerical results obtained with the LTS scheme on a the same grid, now supplied with the splitting wave treatment. Different CFL values have been used and are summarized in Table 1. The number of time steps used to compute the numerical solution and the number of pieces N_p the discontinuity has been split into are also indicated.

The larger the CFL value is, the more accurate the numerical solution is. Moreover, there is no upper bound in the choice of the CFL value. Only one time step can provide the exact solution.

	CFL value	**Time steps (TS)**	$\mathbf{N_p}$
No splitting waves	1.0	20	-
	2.0	10	-
	4.0	5	-
	10.0	2	-
	20.0	1	-
Splitting waves	1.0	20	1
	2.0	10	2
	4.0	5	3
	10.0	2	7
	20.0	1	15

Table 1: Summary of numerical solutions

2.3. Non-linear scalar equation with source terms

Consider now the nonlinear scalar equation with source terms:

$$\frac{\partial u}{\partial t} + \frac{\partial f(u)}{\partial x} = s \tag{25}$$

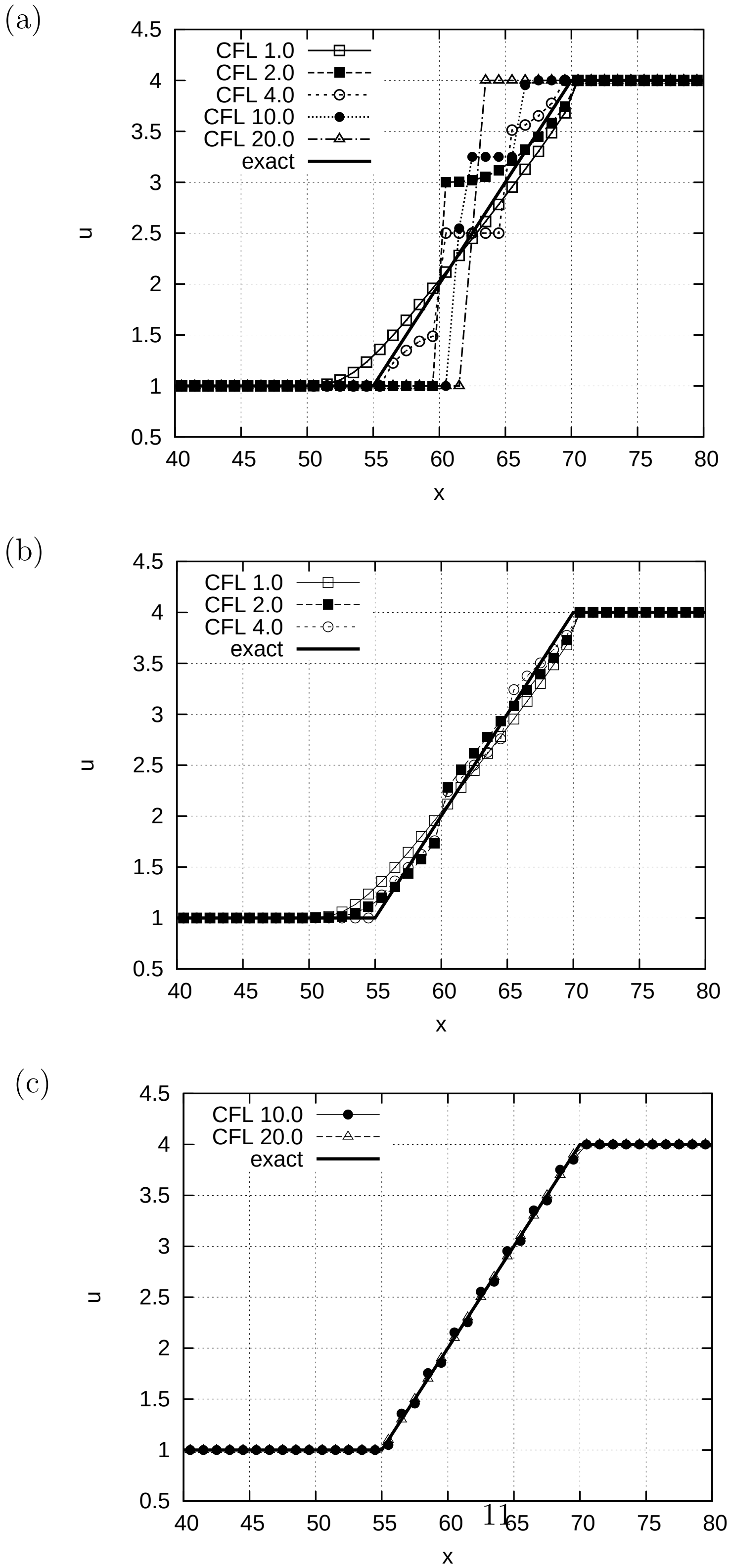

Figure 7: Exact and numerical solution of (16) (a) No splitting rarefaction wave; (b),(c) Splitting rarefaction wave

where s is a source term and the local RP:

$$u(x,0) = \begin{cases} u_L = u_i & if \quad x < 0 \\ u_R = u_{i+1} & if \quad x > 0 \end{cases} \tag{26}$$

According to Roe's approach, the solution of the RP is achieved from an approximate solution $\hat{u}(x,t)$ of the locally linearized problem that must fulfil the Consistency Condition [9]. Integrating over a suitable control volume $[-\frac{\Delta x}{2}, \frac{\Delta x}{2}] \times [0, \Delta t]$

$$\int_{\frac{-\Delta x}{2}}^{\frac{\Delta x}{2}} \hat{u}(x,\Delta t) dx = \Delta x \; (u_{i+1}^n + u_i^n) - (f(u_{i+1}^n) - f(u_i^n))\Delta t + s_{i+1/2}\Delta t \tag{27}$$

For the last integral involving the source term s, the following linearization is assumed

$$s_{i+1/2} = \int_{\frac{-\Delta x}{2}}^{\frac{\Delta x}{2}} s(x,0)\, dx \tag{28}$$

Following [12], a weak solution of the linear RP in (25),(26) that satisfies (27) in the case $\widetilde{\lambda}_{i+1/2} > 0$ was proposed [12]:

$$\hat{u}(x,t) = \begin{cases} u_i & if & x < 0 \\ u_{i+1}^{**} & if & 0 < x < \widetilde{\lambda}_{i+1/2}\, t \\ u_{i+1} & if & x > \widetilde{\lambda}_{i+1/2}\, t \end{cases} \tag{29}$$

where $\widetilde{\lambda}$ is the advection velocity as in (15). Note that one wave is associated to the celerity $\widetilde{\lambda}$ and the other wave is steady and also that

$$u_{i+1}^{**} = u_{i+1} - (\widetilde{\theta}\delta u)_{i+1/2} \tag{30}$$

with

$$\widetilde{\theta}_{i+1/2} = 1 - \frac{s_{i+1/2}}{f(u_{i+1}) - f(u_i)} \tag{31}$$

measuring the relative influence of the source and flux terms
Figure 8 is a sketch of the approximate solution when $\widetilde{\lambda}_{i+1/2} > 0$.

In case that $\widetilde{\lambda}_{i+1/2} < 0$, the procedure is analogous, and the approximate solution is:

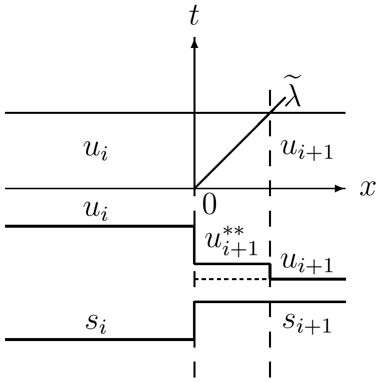

Figure 8: Approximate solution for $\hat{u}(x,t)$.

$$\hat{u}_{(}x,t) = \begin{cases} u_i & if \quad x < \widetilde{\lambda}_{i+1/2}\, t \\ u_i^* & if \quad \widetilde{\lambda}_{i+1/2}\, t < x < 0 \\ u_{i+1} & if \quad x > 0 \end{cases} \tag{32}$$

with

$$u_i^* = u_i + (\widetilde{\theta}\delta u)_{i+1/2} \tag{33}$$

Therefore, the LTS scheme could be written as follows:

If $\widetilde{\lambda}_{i+1/2} > 0$

$$\begin{array}{ll} (\widetilde{\theta}\ \delta u)_{i+1/2} & \text{updates } i+1, \cdots, i+\mu_{i+1/2} \\ (\nu-\mu)_{i+1/2}\ (\widetilde{\theta}\ \delta u)_{i+1/2} & \text{updates } i+\mu_{i+1/2}+1 \end{array} \tag{34}$$

If $\widetilde{\lambda}_{i+1/2} < 0$

$$\begin{array}{ll} (\widetilde{\theta}\ \delta u)_{i+1/2} & \text{updates } i, \cdots, i+\mu_{i+1/2} \\ |\nu-\mu|_{i+1/2}\ (\widetilde{\theta}\ \delta u)_{i+1/2} & \text{updates } i+\mu_{i+1/2} \end{array} \tag{35}$$

where $\nu_{i+1/2} = \dfrac{\widetilde{\lambda}\Delta t}{\Delta x}$ and $\mu_{i+1/2} = int(\nu_{i+1/2})$

2.3.1. First approach: application to Burger's equation with source terms

Consider Burgers's equation including source terms as in [12]:

$$\frac{\partial u}{\partial t} + \frac{1}{2}\frac{\partial u^2}{\partial x} = -u\frac{\partial z}{\partial x} \tag{36}$$

with the initial data

$$u(x,0) = u_o(x) = \begin{cases} u_L & if \quad x < 0 \\ u_R & if \quad x > 0 \end{cases} \qquad z(x) = \begin{cases} z_L & if \quad x < 0 \\ z_R & if \quad x > 0 \end{cases} \tag{37}$$

The same RP in [12] are going to be presented here, using $\Delta x = 1$ at $t = 15s$. The source term discretization used is

$$s_{i+1/2} = -\frac{1}{2}(u_{i+1} + u_i)(z_{i+1} - z_i) \tag{38}$$

All the cases are summarized in Table 2. More information about the nature and the exact solution of each test case can be found in [12].

Table 2: Summary of test cases.

Test case	u_L	u_R	z_L	z_R
1	2.0	1.0	0.0	0.5
2	2.0	1.0	0.0	-0.5
3	1.0	2.0	0.5	0.0
4	1.0	2.0	0.0	0.5
5	2.0	1.0	0.0	1.5
6	1.0	2.0	1.5	0.0

Figures 9–11 plot the results for each test case using different values of CFL. The source term is represented in dashed line, the numerical solutions with CFL=1 using ($-\triangle-$), the numerical solution with CFL=5 using ($-\square-$) and that with CFL=30 using ($-\circ-$). They are compared with the exact solution (—). Note that CFL=30 is the largest value possible leading to one single time step. As can be observed, these test cases are very extreme, particularly the cases 5 and 6 where the source term dominate the convective term. The numerical solution from the LTS scheme when using CFL>1 is able to approximate the classical upwind explicit (CUE) scheme using

CFL=1, mainly in the test cases 1,2,3 and 4, but is not able to approximate the exact solution in a single time step. The main advantage of the LTS scheme is that the time step is not restricted by the CFL condition allowing large Δt values. From CUE, the speed celerity $\widetilde{\lambda}$ is estimated as in the homogeneous case (15). The fact is that, in several situations with large source terms that influence the convective term, using the LTS scheme, this linearization could leads to a wrong solution because of an overestimation or underestimation of this value. A way to overcome this situation is proposed.

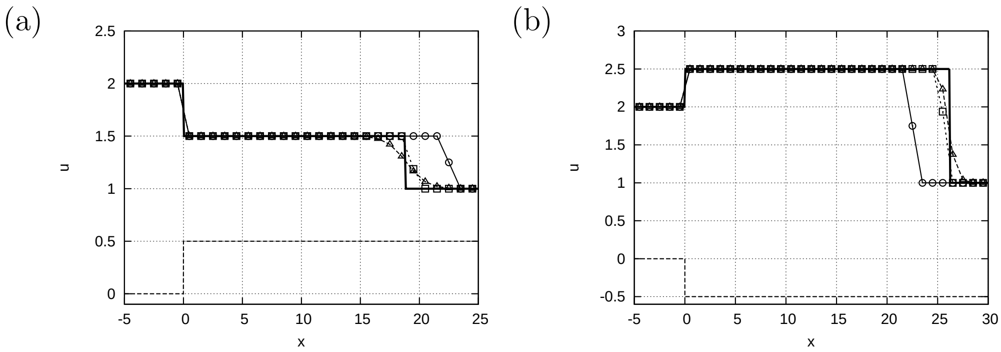

Figure 9: Exact (——) and computed solutions at $t = 15s$ for (a) test case 1 and (b) test case 2 using CFL=1 ($-\triangle-$), CFL=5 ($-\square-$) and CFL=30 ($-\circ-$)

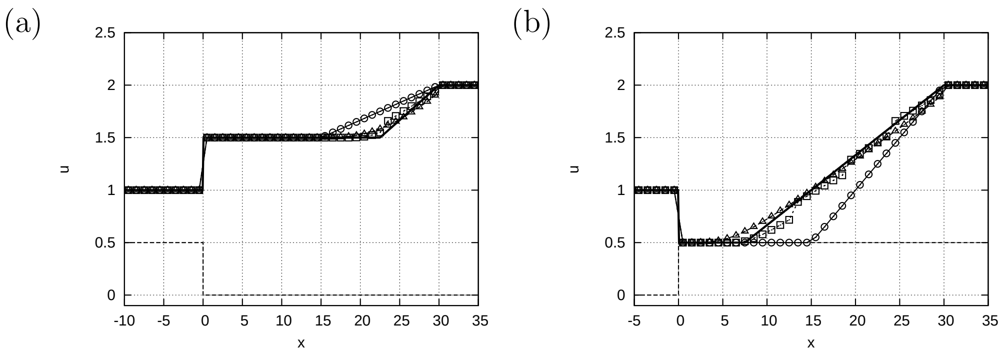

Figure 10: Exact (——) and computed solutions at $t = 15s$ for (a) test case 3 and (b) test case 4 using CFL=1 ($-\triangle-$), CFL=5 ($-\square-$) and CFL=30 ($-\circ-$)

2.3.2. Accurate estimation of the wave celerity

Let s_e be the exact value of the integral of the source term in the control volume

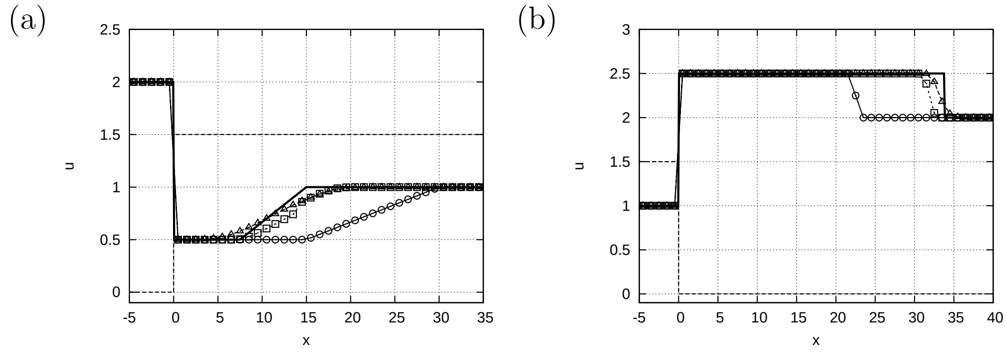

Figure 11: Exact (——) and computed solutions at $t = 15s$ for (a) test case 5 and (b) test case 6 using CFL=1 ($-\triangle-$), CFL=5 ($-\square-$) and CFL=30 ($-\circ-$)

$$s_e = \int_0^{\Delta t} \int_{\frac{-\Delta x}{2}}^{\frac{\Delta x}{2}} s \, dx \, dt \tag{39}$$

A better wave celerity $\hat{\lambda}_{i+1/2}$ can be estimated by using directly the information provided by the analytical solution, constructed by means of the appropriate Rankine-Hugoniot (hereafter RH) conditions.

Assuming the RP in (26), a weak solution satisfying (27) for the case $\hat{\lambda}_{i+1/2} > 0$ is proposed (the case $\hat{\lambda}_{i+1/2} < 0$ is analogous):

$$\hat{u}(x,t) = \begin{cases} u_i & if \quad x < 0 \\ u_{i+1}^{**} & if \quad 0 < x < \hat{\lambda}_{i+1/2}\, t \\ u_{i+1} & if \quad x > \hat{\lambda}_{i+1/2}\, t \end{cases} \tag{40}$$

Figure 12 is a sketch of the approximate solution in this situation. Enforcing Rankine-Hugoniot conditions across the two waves:

$$\begin{cases} f(u_{i+1}) - f(u_{i+1}^{**}) = \hat{\lambda}_{i+1/2}(u_{i+1} - u_{i+1}^{**}) \\ f(u_{i+1}^{**}) - f(u_i) - s_e = \lambda_s(u_{i+1}^{**} - u_i) = 0 \end{cases} \tag{41}$$

where $\lambda_s = 0$ is the wave celerity associated to the steady discontinuity at $x = 0$. The first RH condition leads to:

$$\hat{\lambda}_{i+1/2} = \frac{f(u_{i+1}) - f(u_{i+1}^{**})}{u_{i+1} - u_{i+1}^{**}} \tag{42}$$

In order to apply the method described in (34) and (35), the consistency condition using the exact integration of the source term over the control

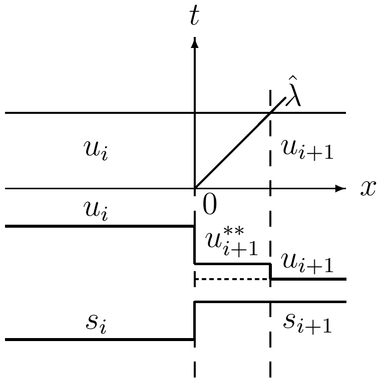

Figure 12: Approximate solution for $\hat{u}(x,t)$.

volume (27) must be checked. Taking into account the second RH condition in (41) :

$$s_e = f(u^{**}_{i+1}) - f(u_i) \tag{43}$$

Using definitions (30), (42) and (43):

$$\hat{\lambda}_{i+1/2}\ \widetilde{\theta}_{i+1/2}\ \delta u = \hat{\lambda}_{i+1/2}\left(\frac{u_{i+1} - u^{**}_{i+1}}{\delta u}\right)\delta u = \frac{f(u_{i+1}) - f(u^{**}_{i+1})}{u_{i+1} - u^{**}_{i+1}}(u_{i+1} - u^{**}_{i+1}) =$$
$$f(u_{i+1}) - f(u^{**}_{i+1}) - f(u_i) + f(u_i) = \delta f_{i+1/2} - s_e \tag{44}$$

Hence the consistency of our numerical scheme is proved. Next step is to replace $\widetilde{\lambda}$ by $\hat{\lambda}$ in (34) and (35) leading the following algorithm:

If $\hat{\lambda}_{i+1/2} > 0$

$$\begin{array}{ll} (\widetilde{\theta}\ \delta u)_{i+1/2} & \text{updates } i+1, \cdots, i+\mu_{i+1/2} \\ (\nu - \mu)_{i+1/2}\ (\widetilde{\theta}\ \delta u)_{i+1/2} & \text{updates } i+\mu_{i+1/2}+1 \end{array} \tag{45}$$

If $\hat{\lambda}_{i+1/2} < 0$

$$\begin{array}{ll} (\widetilde{\theta}\ \delta u)_{i+1/2} & \text{updates } i, \cdots, i+\mu_{i+1/2} \\ |\nu-\mu|_{i+1/2}\ (\widetilde{\theta}\ \delta u)_{i+1/2} & \text{updates } i+\mu_{i+1/2} \end{array} \quad (46)$$

where $\nu_{i+1/2} = \dfrac{\hat{\lambda}\Delta t}{\Delta x}$ and $\mu_{i+1/2} = int(\nu_{i+1/2})$

2.3.3. Second approach: application to the Burgers equation with source terms

Considering (36), the RP in (37) and the test cases in table 2, the performance of the first and second approaches of the wave celerity is evaluated at $t = 15s$ and computed with $\Delta x = 1$.

The same source term discretization as in (38) is used, representing it in dashed line. The numerical solutions with CFL=1 ($-\triangle-$), with CFL=30 using $\widetilde{\lambda}$ as wave celerity ($-\circ-$) and with CFL=30 using $\hat{\lambda}$ as wave celerity ($-\bullet-$) are going to be compared with the exact solution (——). Also the splitting rarefaction treatment as explained before has been used for computing the numerical solutions with the LTS scheme.

Figures 13–15 show the results for all test cases. The main conclusion is that the LTS scheme, including a good source term treatment is less diffusive than the conventional explicit upwind scheme and it can be able to reproduce the exact solution. However, if no correction in the estimation of the wave celerity is applied, the numerical solution is not able to approximate the exact solution. Maybe, when using the CUE scheme there is no noticeable difference between the two approaches of the wave celerity, because the method is forced to work with small time steps but the LTS scheme allows larger time steps, and therefore important error is introduced if a careless estimation of the wave celerity is applied. Note that this improvement has been possible in the particular case of a scalar equation with known exact solution.

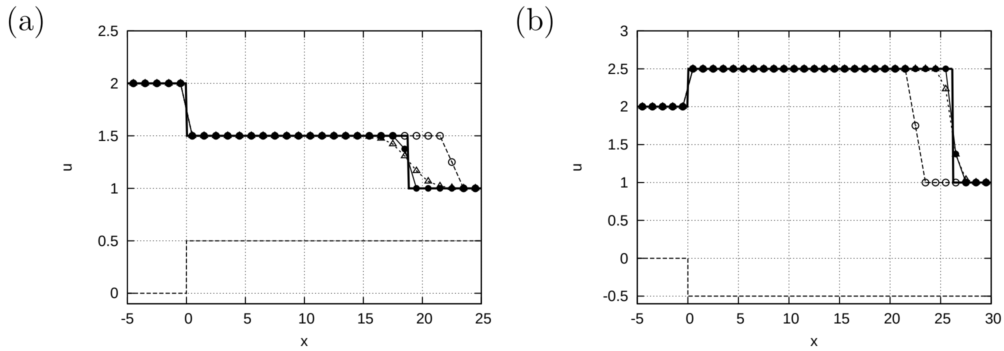

Figure 13: Exact (——) and computed solutions at $t = 15s$ for (a) test case 1, and (b) test case 2 using CFL=1 ($-\triangle-$), CFL=30 with $\widetilde{\lambda}$ as wave celerity ($-\circ-$) and CFL=30 with $\hat{\lambda}$ as wave celerity ($-\bullet-$)

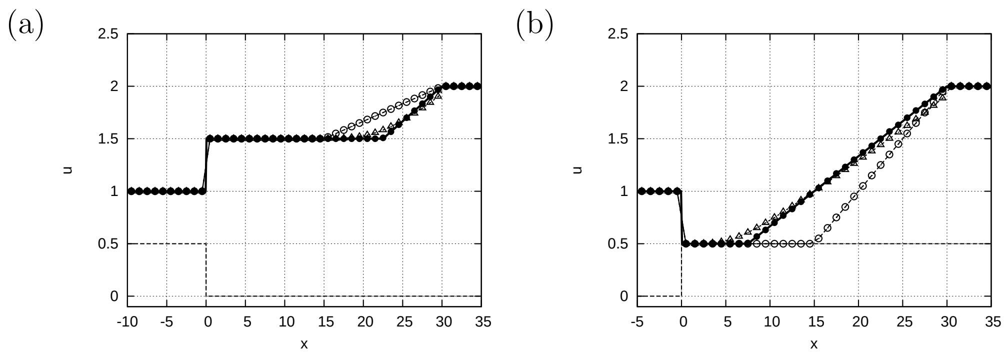

Figure 14: Exact (——) and computed solutions at $t = 15s$ for (a) test case 3, and (b) test case 4 using CFL=1 ($-\triangle-$), CFL=30 with $\widetilde{\lambda}$ as wave celerity ($-\circ-$) and CFL=30 with $\hat{\lambda}$ as wave celerity ($-\bullet-$)

3. System of conservation laws with source terms

The extension of the proposed LTS scheme to systems of equations with source terms is discussed in this section. A 2x2 hyperbolic nonlinear system of equations can be expressed in the form

$$\frac{\partial \mathbf{U}}{\partial t} + \frac{\partial \mathbf{F}}{\partial x} = \mathbf{S} \tag{47}$$

where $\mathbf{U}$ is the vector of conserved variables, $\mathbf{F}$ is the vector of fluxes of these conserved variables and $\mathbf{S}$ represents the vector of source terms. A Jacobian matrix $\mathbf{J}$ can be defined

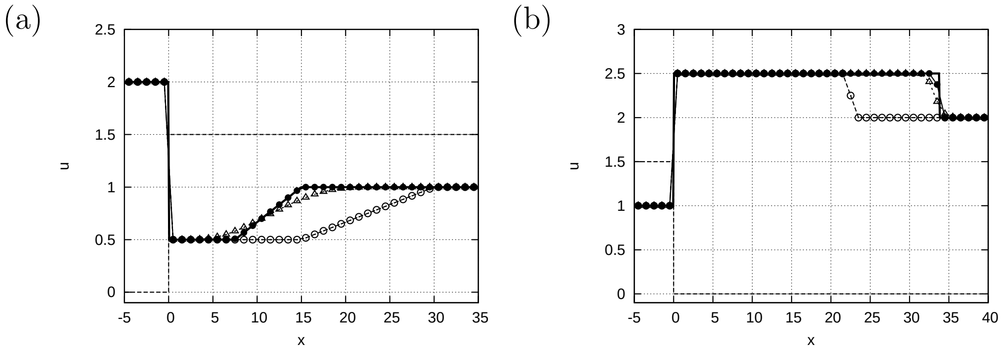

Figure 15: Exact (—–) and computed solutions at $t = 15s$ for (a) test case 5, and (b) test case 6 using CFL=1 ($-\triangle-$), CFL=30 with $\widetilde{\lambda}$ as wave celerity ($-\circ-$) and CFL=30 with $\hat{\lambda}$ as wave celerity ($-\bullet-$)

$$\mathbf{J} = \frac{d\mathbf{F}}{d\mathbf{U}} \tag{48}$$

The strictly hyperbolicity property of the system ensures that the two eigenvalues λ^1, λ^2 of the Jacobian are real and different and it is possible to define two matrices $\mathbf{P} = (\mathbf{e}^1, \mathbf{e}^2)$ and $\mathbf{P}^{-1}$, with $\mathbf{e}^1, \mathbf{e}^2$ the eigenvectors of $\mathbf{J}$, achieving the diagonalization:

$$\mathbf{J} = \mathbf{P}\mathbf{\Lambda}\mathbf{P}^{-1} \tag{49}$$

Considering a RP with initial values $\mathbf{U}_i, \mathbf{U}_{i+1}$:

$$\mathbf{U}(x,0) = \begin{cases} \mathbf{U}_i & if \quad x < 0 \\ \mathbf{U}_{i+1} & if \quad x > 0 \end{cases} \tag{50}$$

Let Δt be the time step. Now, integrating (47) over a suitable control volume $[-X, X]$ where

$$-X \leq X_{min}, \quad X \geq X_{max} \tag{51}$$

and X_{min}, X_{max} are the positions of the minimum and the maximum wave celerities at $t = \Delta t$

$$\int_{-X}^{+X} \hat{\mathbf{U}}(x,\Delta t)\, dx = X\left(\mathbf{U}_{i+1} + \mathbf{U}_i\right) - \left(\mathbf{F}(\mathbf{U}_{i+1}) - \mathbf{F}(\mathbf{U}_i)\right)\Delta t + \mathbf{S}_{i+1/2}\Delta t \tag{52}$$

where $\hat{\mathbf{U}}(x,t)$ is the approximate solution of the locally linearized RP. The source term can be linearized following [12] as follows:

$$\mathbf{S}_{i+1/2} = \int_{-X}^{+X} \mathbf{S}(x,0)\, dx \tag{53}$$

Following [12] a three wave approximate solution can be built from (52). $\widehat{\mathbf{U}}(x,t)$ is governed by the celerities $\widetilde{\lambda}^1$, $\widetilde{\lambda}^2$ and consists of four regions. Depending on the flow conditions (subcritical or supercritical) three situations can be found. More details of the approximate Riemann solutions for each case can be found in [12] . Figure 16 shows the subcritical case:

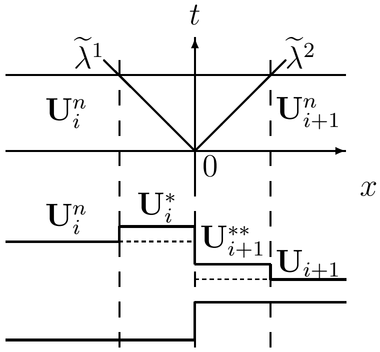

Figure 16: Values of the solution $\mathbf{U}$ in each wedge of the (x,t) plane for the subcritical case.

Provided that Roe's linearization [14] is used to uncouple the homogeneous part of the system, an approximate Jacobian matrix $\tilde{\mathbf{J}}_{i+1/2}$ can be built whose eigenvalues $\widetilde{\lambda}^1, \widetilde{\lambda}^2$ and eigenvectors $\widetilde{\mathbf{e}}^1, \widetilde{\mathbf{e}}^2$ satisfy:

$$\widetilde{\mathbf{J}}_{i+1/2} = \widetilde{\mathbf{P}}_{i+1/2} \widetilde{\mathbf{\Lambda}}_{i+1/2} \widetilde{\mathbf{P}}^{-1}_{i+1/2} \tag{54}$$

where $\widetilde{\mathbf{P}} = (\widetilde{\mathbf{e}}^1, \widetilde{\mathbf{e}}^2)$ and $\widetilde{\mathbf{\Lambda}}_{i+1/2}$ is a diagonal matrix with eigenvalues $\widetilde{\lambda}^m_{i+1/2}$ in the main diagonal:

$$\widetilde{\mathbf{\Lambda}}_{i+1/2} = \begin{pmatrix} \widetilde{\lambda}^1 & 0 \\ 0 & \widetilde{\lambda}^2 \end{pmatrix}_{i+1/2} \tag{55}$$

Following a flux difference procedure, the difference in vector $\mathbf{U}$ across the grid edge is projected onto the matrix eigenvector basis and the same for the source term:

$$\delta \mathbf{U}_{i+1/2} = \sum_{m=1}^{2} (\alpha\ \widetilde{\mathbf{e}})^m_{i+1/2} \qquad \mathbf{S}_{i+1/2} = \sum_{m=1}^{2} (\beta\ \widetilde{\mathbf{e}})^m_{i+1/2} \tag{56}$$

Therefore:

$$(\delta \mathbf{F} - \mathbf{S})_{i+1/2} = (\widetilde{\mathbf{J}}\delta \mathbf{U} - \mathbf{S})_{i+1/2} = \sum_{m=1}^{2} \left(\widetilde{\lambda}^* \alpha \widetilde{\mathbf{e}}\right)^m_{i+1/2} \tag{57}$$

where

$$\widetilde{\lambda}^{*,m}_{i+1/2} = \widetilde{\lambda}^m_{i+1/2}\ \theta^m_{i+1/2} \qquad \theta^m_{i+1/2} = \left(1 - \frac{\beta}{\widetilde{\lambda}\alpha}\right)^m_{i+1/2} \tag{58}$$

being $\theta^m_{i+1/2}$ the parameter expressing the influence of the source term over that of the flux difference.

Therefore, the LTS scheme can be formulated for systems of equations as follows:

If $\widetilde{\lambda}_{i+1/2} > 0$

$$\begin{array}{ll} (\gamma\ \widetilde{\mathbf{e}})^m_{i+1/2} & \text{updates } i+1, \cdots, i+\mu_{i+1/2} \\ (\nu - \mu)^m_{i+1/2}\, (\gamma\ \widetilde{\mathbf{e}})^m_{i+1/2} & \text{updates } i+\mu_{i+1/2}+1 \end{array} \tag{59}$$

If $\widetilde{\lambda}_{i+1/2} < 0$

$$\begin{array}{ll} (\gamma\ \widetilde{\mathbf{e}})^m_{i+1/2} & \text{updates } i, \cdots, i+\mu_{i+1/2} \\ |\nu - \mu|^m_{i+1/2}\, (\gamma\ \widetilde{\mathbf{e}})^m_{i+1/2} & \text{updates } i+\mu_{i+1/2} \end{array} \tag{60}$$

where $\nu^m_{i+1/2} = \dfrac{\Delta t}{\Delta x} \widetilde{\lambda}^m_{i+1/2}$, $\mu^m_{i+1/2} = int(\nu^m_{i+1/2})$ and $\tilde{\gamma}^m_{i+1/2} = (\tilde{\alpha}\tilde{\theta})^m_{i+1/2}$

4. Application to the 1D shallow water equations

4.1. Equations

The 1D shallow water mass and momentum system can be written:

$$\mathbf{U} = \begin{pmatrix} A \\ Q \end{pmatrix}, \quad \mathbf{F} = \begin{pmatrix} Q \\ \frac{Q^2}{A} + gI_1 \end{pmatrix} \quad \mathbf{S} = \begin{pmatrix} 0 \\ g\left[I_2 + A\left(S_0 - S_f\right)\right] \end{pmatrix} \tag{61}$$

where Q is the discharge, A is the wetted cross section, g is the acceleration due to the gravity, S_0 is the bed slope

$$S_0 = -\frac{\partial z_b}{\partial x} \tag{62}$$

S_f is the friction slope here represented by the empirical Manning law

$$S_f = \frac{Q^2}{n^2 A^2 R^{4/3}} \tag{63}$$

where R is the hydraulic radius and n is the Manning's roughness coefficient. I_1 represents a hydrostatic pressure force term

$$I_1 = \int_{z_b}^{z_s} (h - \eta)\sigma(x, \eta)\; d\eta \tag{64}$$

in a section of water level z_s, bed level z_b and width $\sigma(x, \eta)$. On the other hand, I_2 accounts for the pressure force due to the longitudinal width variations:

$$I_2 = \int_{z_b}^{z_s} (h - \eta)\frac{\partial b(x, \eta)}{\partial x}\; d\eta \tag{65}$$

The approximate Jacobian $\widetilde{\mathbf{J}}$ is

$$\tilde{\mathbf{J}}_{i+1/2} = \begin{pmatrix} 0 & 1 \\ \widetilde{c}^2 - \widetilde{u}^2 & 2\widetilde{u} \end{pmatrix}_{i+1/2} \tag{66}$$

with [15]

$$\widetilde{c} = \sqrt{g\frac{(A/b)_i + (A/b)_{i+1}}{2}} \quad \widetilde{u} = \frac{Q_{i+1}\sqrt{A_{i+1}} + Q_i\sqrt{A_i}}{\sqrt{A_{i+1}} + \sqrt{A_i}} \tag{67}$$

where $b = \sigma(x, h)$. The resulting set of approximate eigenvalues and eigenvectors is

$$\begin{gathered} \widetilde{\lambda}^1 = \widetilde{u} - \widetilde{c} \qquad \widetilde{\lambda}^2 = \widetilde{u} + \widetilde{c} \\ \widetilde{\mathbf{e}}^1 = \begin{pmatrix} 1 \\ \widetilde{u} - \widetilde{c} \end{pmatrix} \qquad \widetilde{\mathbf{e}}^2 = \begin{pmatrix} 1 \\ \widetilde{u} + \widetilde{c} \end{pmatrix} \end{gathered} \tag{68}$$

4.2. Rarefaction splitting treatment

Using the LTS scheme (59), (60), when a rarefaction appears in the context of the shallow water equations, it can be split in several waves travelling at different speeds ensuring exact conservation in the sense of Roe. This is demonstrated here in the particular case of a rarefaction wave split in two pieces.

When representing a rarefaction through a unique wave $\tilde{\lambda}$ at interface $i+1/2$, the quantity $(\nu\gamma\tilde{e})_{i+1/2} = \dfrac{\tilde{\lambda}_{i+1/2}\Delta t}{\Delta x}(\gamma\tilde{e})_{i+1/2}$ is sent. The aim of the splitting is originating two waves, $\tilde{\lambda}^a_{i+1/2}$ and $\tilde{\lambda}^b_{i+1/2}$, that, in order to be conservative verify

$$\frac{\tilde{\lambda}_{i+1/2}\Delta t}{\Delta x}(\gamma\tilde{e})_{i+1/2} = \frac{\tilde{\lambda}^a_{i+1/2}\Delta t}{\Delta x}(\gamma^a\tilde{e})_{i+1/2} + \frac{\tilde{\lambda}^b_{i+1/2}\Delta t}{\Delta x}(\gamma^b\tilde{e})_{i+1/2} \tag{69}$$

Therefore enforcing

$$(\tilde{\lambda}\gamma)_{i+1/2} = (\tilde{\lambda}^a\gamma^a)_{i+1/2} + (\tilde{\lambda}^b\gamma^b)_{i+1/2} \tag{70}$$

According to (70), the definition of $\gamma^a_{i+1/2}$ and $\gamma^b_{i+1/2}$ follows

$$\gamma^a_{i+1/2} = \gamma_{i+1/2}\left(\frac{\tilde{\lambda}^b - \tilde{\lambda}}{\tilde{\lambda}^b - \tilde{\lambda}^a}\right)_{i+1/2} \qquad \gamma^b_{i+1/2} = \gamma_{i+1/2}\left(\frac{\tilde{\lambda} - \tilde{\lambda}_a}{\tilde{\lambda}^b - \tilde{\lambda}^a}\right)_{i+1/2} \tag{71}$$

There is some freedom for the choice of $\tilde{\lambda}^a_{i+1/2}$ and $\tilde{\lambda}^b_{i+1/2}$ for example, they could be defined as follows:

$$\tilde{\lambda}^a_{i+1/2} = \varepsilon\,(\lambda_i + \tilde{\lambda}_{i+1/2}) \qquad \tilde{\lambda}^b_{i+1/2} = (1-\varepsilon)\,(\lambda_{i+1} + \tilde{\lambda}_{i+1/2}) \tag{72}$$

where ε is a free parameter. In this case, $\varepsilon = 0.5$ has been chosen. The number of pieces N_p that the rarefaction is split into is again related with the wave strength. In this work, the choice is related with the integer part of $\dfrac{\gamma_{i+1/2}\ \Delta t}{\Delta x}$.

In order to see the performance of this technique when dealing with a rarefaction, a flat frictionless rectangular channel 100 m long, 1 m wide, with initial conditions of zero velocity and a discontinuity in the water level surface

$$h(x, t = 0) = \begin{cases} 4m & \text{if} \quad x < 50\text{m} \\ 1m & \text{if} \quad x > 50\text{m} \end{cases} \tag{73}$$

is considered. Two numerical solutions using the LTS scheme computed with CFL=5.0 and $\Delta x = 1.0m$ are compared with the exact solution (——). The results from the LTS scheme with rarefaction splitting are plotted using $(- \bullet -)$, those from the LTS without splitting are plotted using $(- \circ -)$ in Figure 17 (a) and (b) for the water depth and discharge respectively after $t = 3s$. Although oscillations appear in the presence of the shock wave in both numerical solutions, the LTS scheme using the split rarefactions is more accurate than the LTS scheme without the splitting treatment.

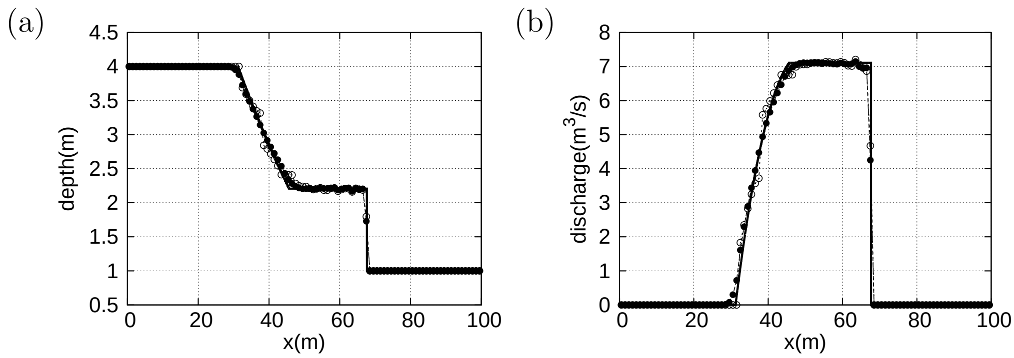

Figure 17: (a) Exact (——) and numerical solutions at $t = 3s$ for (a) the height, and (b) the discharge using splitting $(- \bullet -)$ and no splitting $(- \circ -)$ rarefaction treatment

4.3. Boundary conditions

The boundary conditions dicretization is another issue of importance and requires a careful consideration. In the context of the shallow water equations, open boundaries and closed boundaries can appear and are going to be analyzed.

In the case of open boundaries, two flow situations can be distinguished: subcritical and supercritical. When dealing with a supercritical outlet boundary, no external information is required. In fact, the boundary cell receives the information coming from the inner cells according to the scheme provided in (59) and (60). If some of the contributions cross the boundary they are stored at inlet and outlet 'bags' in order to control conservation but they do not affect the updated solution of the boundary cell (Figure 18).

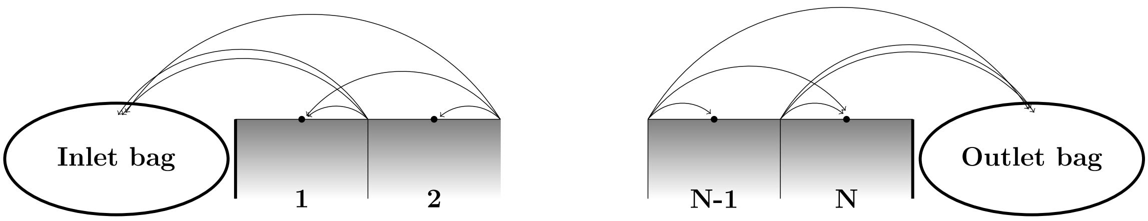

Figure 18: Open boundaries in the LTS scheme

In case of having subcritical inlet or outlet boundary, one variable is externally imposed as physical boundary conditions and the other variable is calculated using the updating information arriving from the inner interfaces. Also some of the contributions cross the boundary, so they are stored as in the supercritical case.

At closed boundaries, two possible techniques are proposed: an accumulation technique and a reflection technique. Consider the downstream boundary at node N (the reasoning for the upstream boundary is analogous) and the information from edge *i+1/2* ($\widetilde{\lambda}_{i+1/2} > 0$). If $i + \mu_{i+1/2} + 1 \ > \ N$, some of the contributions from *i+1/2* go out of the downstream end of the domain. As the solid wall condition requires that no information crosses the boundary and the method must remain conservative, the accumulation technique stores these contributions at the downstream boundary cell N as shown in Figure 19 (a). On the other hand, the reflection technique considers the downstream outlet edge as a mirror, sending the information that would cross the boundary back to the corresponding cell. It can be seen in Figure 19 (b).

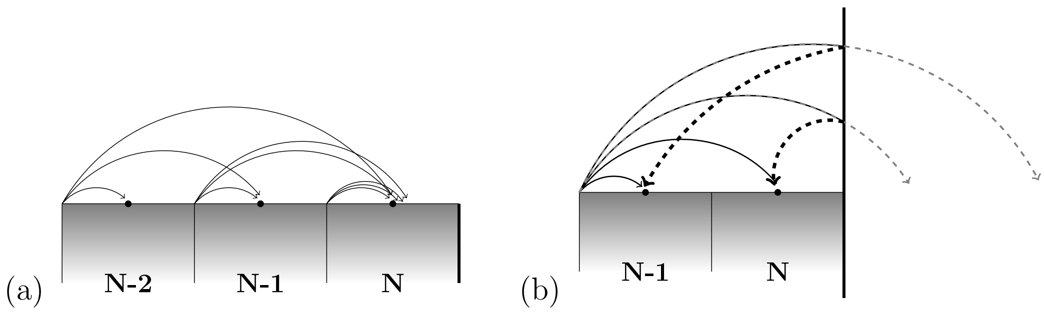

Figure 19: Boundary treatment: (a) Accumulation technique and (b) Reflection technique

The reflection technique is preferred here because the LTS scheme using very large CFL numbers in closed boundaries could lead the boundary cells to accumulate excessive information in a time step producing oscillations and non-physical situations. In order to justify this choice, the same dambreak problem proposed in (73) is used considering solid walls at $x = 0\ m$ and at $x = 100\ m$. After several seconds the shock and the rarefaction waves arrive to the end of the domain and rebound. The numerical solutions with the LTS scheme are computed again with CFL=5.0 and $\Delta x = 1.0m$. The two ways of dealing with the closed boundaries, accumulation $(- \circ -)$ and reflection $(- \bullet -)$ technique are compared with the exact solution (——) at t=10.5s (Figure 20 (a) for the height and (b) for the discharge) and at t=16.5s (Figure 21 (a) for the height and (b) for the discharge). The results highlight that the reflection technique achieves more accurate solutions than the accumulation technique mainly near the time when the waves collide with the solid walls. After the reflection, the two techniques provide similar results.

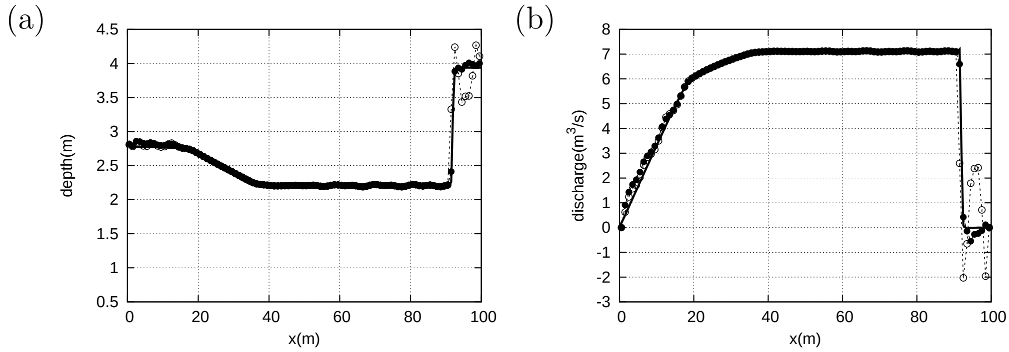

Figure 20: (Exact (——) and numerical solutions at $t = 10.5s$ for (a) the depth, and (b) the discharge using the accumulation $(- \circ -)$ and reflection $(- \bullet -)$ technique

4.4. Entropy fix, source terms and the CFL limit

The LTS scheme formulated in this work is actually an alteration of the basic Roe scheme where larger CFL values can be used. As it is well known, the basic explicit scheme requires some kind of correction in order to avoid non-physical situations near sonic points. This correction, called entropy fix, must also be applied in the proposed LTS scheme. In this work, the version of the Harten-Hyman entropy fix [13] has been adopted.

An upwind discretization for the source term related not only with the bed slope but also with the friction term is adopted according to [12] . This

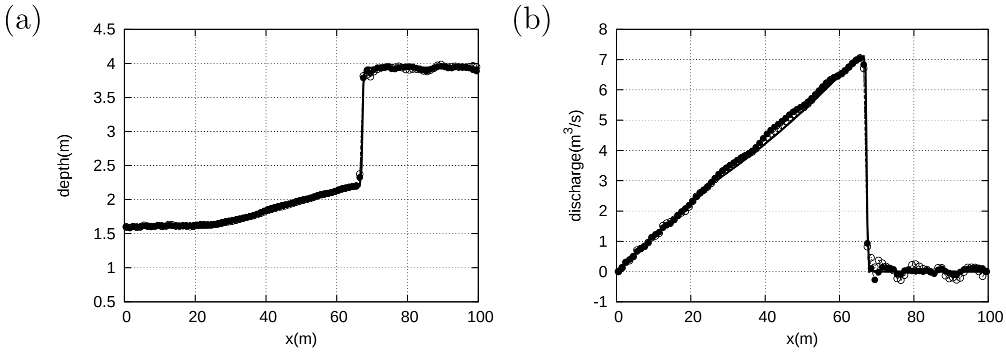

Figure 21: (Exact (——) and numerical solutions at $t = 16.5s$ for (a) the depth, and (b) the discharge using the accumulation ($-\circ-$) and reflection ($-\bullet-$) technique

treatment is able to satisfy the preservation of steady-states such as still water equilibrium in the context of the shallow water equations providing discrete evaluations of the source term that ensure energy dissipating solutions when demanded. Also the wet/dry front has been formulated following [12], avoiding the appearance of negative values of water depth.

A more accurate estimation of the waves celerities in presence of strong source terms or big discontinuities could be based on the three RH conditions associated to the approximate solution from (52) according to the idea suggested in the non-linear scalar case. However, due to the mutual dependence between the waves celerities and the intermediate states $\mathbf{U}^*$ and $\mathbf{U}^{**}$, there is not a simple or straightforward procedure [16] to achieve an accurate solution at very high CFL numbers (associated to only one or two time steps in total). Therefore, instead of seeking a correction in the waves speeds in presence of strong source terms or big discontinuities, the present work is focused on applying a reduction on the CFL value. This is next explained. A parameter that includes the influence not only of the size of the discontinuity in the solution but also of the initial values is considered as proposed in [10]:

$$\xi_1 = \frac{min_i\{|\mathbf{U}_i|, |\mathbf{U}_{i+1}|, |\delta\mathbf{U}_{i+1/2}|\}}{|\delta\mathbf{U}_{i+1/2}|} \qquad 1 \le i \le N \tag{74}$$

where $0 \le \xi_1 \le 1$. Also, a second parameter ξ_2 is defined incorporating the equivalent influence of the bed slope source term as follows:

$$\xi_2 = \frac{min_i\{|d_i|, |d_{i+1}|, |\delta d_{i+1/2}|\}}{|\delta d_{i+1/2}|} \qquad 1 \le i \le N \tag{75}$$

where $0 \leq \xi_2 \leq 1$ and $d = h + z$ is the water surface level. Let ξ be the minimum of these two parameters,

$$\xi = min(\xi_1, \xi_2) \tag{76}$$

If $\mathbf{U}$ or d are gradually varied functions, $\xi = 1$ and the CFL value is not necessary to be diminished. Otherwise, a reduction in the CFL initial value, i.e., in the time step, is required in order to achieve a good solution. In this work, the value $\xi = 0.25$ is proposed as a limit. Under this value, the CFL number will be reduced to 1.0 recovering the original Roe's method and over this value, a linear interpolation between 1.0 and the CFL number chosen initially according to the parameter ξ is submitted. Therefore, the final CFL value (CFL_l) can be expressed as follows:

$$CFL_l = \begin{cases} 1.0 & if \quad \xi \leq 0.25 \\ 1.0 + \dfrac{\mathrm{CFL} - 1.0}{0.75}(\xi - 0.25) & if \quad \xi > 0.25 \end{cases} \tag{77}$$

An alternative way to proceed could be establishing the limit in $\xi = 1.0$. Under this number the CFL value will be reduced to 1.0. Also in the case where flow regime transitions occurs (mainly in hydraulic jumps) the CFL number is reduced to ensure the correct solution of the problem.

4.5. Test cases

4.5.1. Application to steady flow with source terms

MacDonald et al. [17] supplied a set of realistic open channel flow test cases with analytical solution very well suited to validate the numerical schemes. Three examples from [18] are used here. They both apply a Manning friction coefficient $n = 0.03$, have been simulated with $\Delta x = 1.0$ and the inlet discharge is 20 m^3/s. In test case 1 the flow is subcritical all along the 150 m length and the 10 m wide rectangular channel. The downstream boundary condition is a fixed height. The steady water depth is:

$$h(x) = 0.8 + 0.25\ exp\left(33.75\left(\frac{x}{150} - 1/2\right)^2\right) \tag{78}$$

Test case 2 corresponds to a trapezoidal channel with 10 m bottom width and 200 m length. The side slope of the channel is 2, and there is not downstream boundary condition. Hence, a smooth transition between subcritical flow upstream (at the first half of the reach) and supercritical flow downstream (at the second half) takes place. Here, the steady water depth is expressed as follows:

$$h(x) = 0.706033 - 0.25\ tanh\left(\frac{x-100}{50}\right) \tag{79}$$

In test case 3, the 10 m wide rectangular channel steepens and then flattens out again along the 150 m lenght. The solutions changes smoothly from subcritical flow to supercritical flow at $x = 50m$. After it return via a hydraulic jump to subcritical flow at $x = 100m$. The downstream boundary condition is a fixed height of 1.700225 m and the steady water depth is:

$$h(x) = 0.741617 - \frac{0.25}{tanh(3)}\ tanh\left(3\frac{x-50}{50}\right) \tag{80}$$

The results for these test cases can be observed in Figures 22, 23 and 24 where the numerical solution using CFL = 60.0 ($-\circ-$) is compared with the exact solution (—–). Also the bed level is represented in dashed line. The results indicate that the LTS scheme is really valid for computing steady states with very large CFL numbers only accessible for the implicit methods.

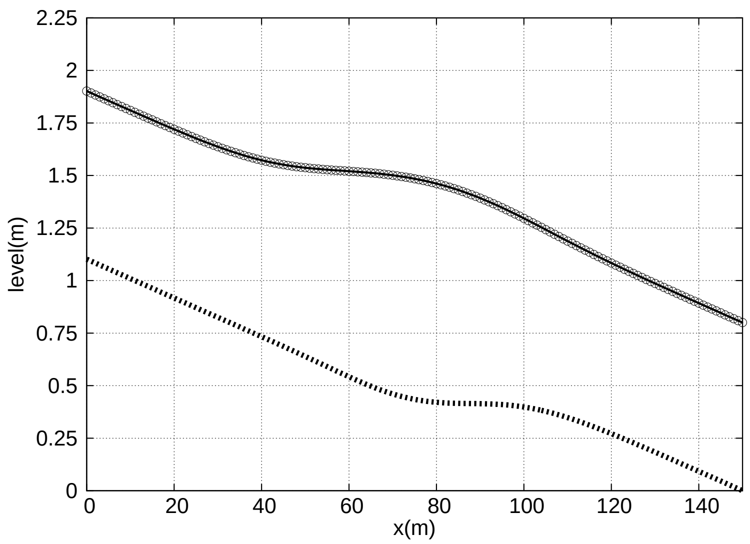

Figure 22: Exact (—–) and numerical ($-\circ-$) solution for Macdonald's test case 1

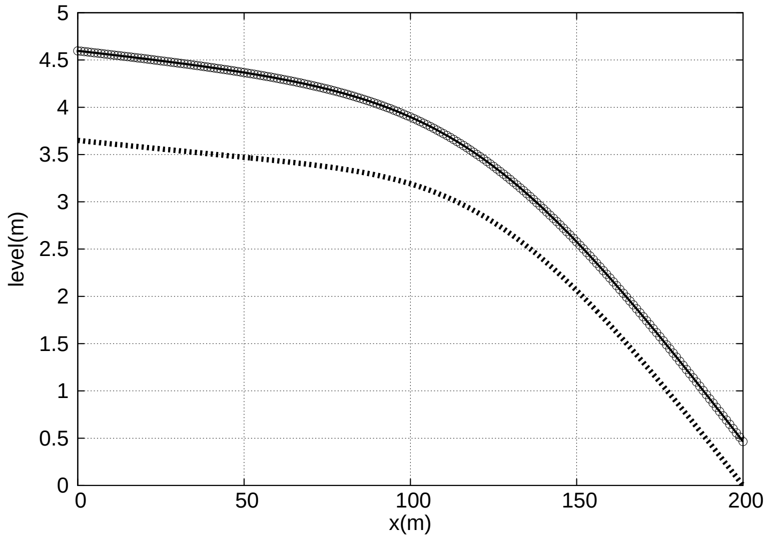

Figure 23: Exact (——) and numerical (− ◦ −) solution for Macdonald's test case 2

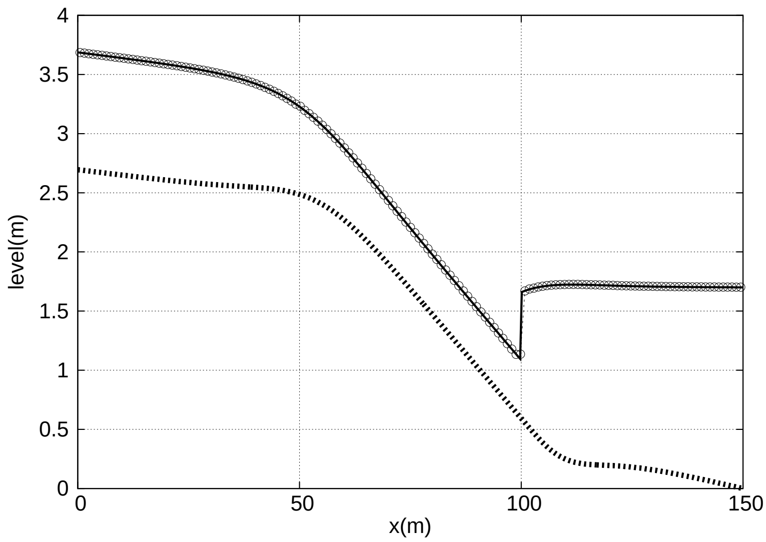

Figure 24: Exact (——) and numerical (− ◦ −) solution for Macdonald's test case 3

The CFL limiter presented before is also activated in order to ensure the correct solution of the numerical approach. Figure 25 provides the information about the evolution of the time step in each test case. The time step value using CFL=1.0 in the test case 1 is near 0.18 in comparison with the

LTS scheme using CFL=60.0 where the time step value is near 8.91. In the second test case, the time step using CFL 1.0 is near 0.16 whereas using CFL=60.0, after several oscillations related with the CFL limiter and the smooth transition, arrives to 7.95 approximately. In test case 3 a hydraulic jump occurs, and the CFL value is suddenly limited to 2.0, so there is no much difference between the time step in the LTS scheme using CFL=60.0 (the actual CFL value used is near 2.0) and the conventional explicit upwind method with CFL=1.0.

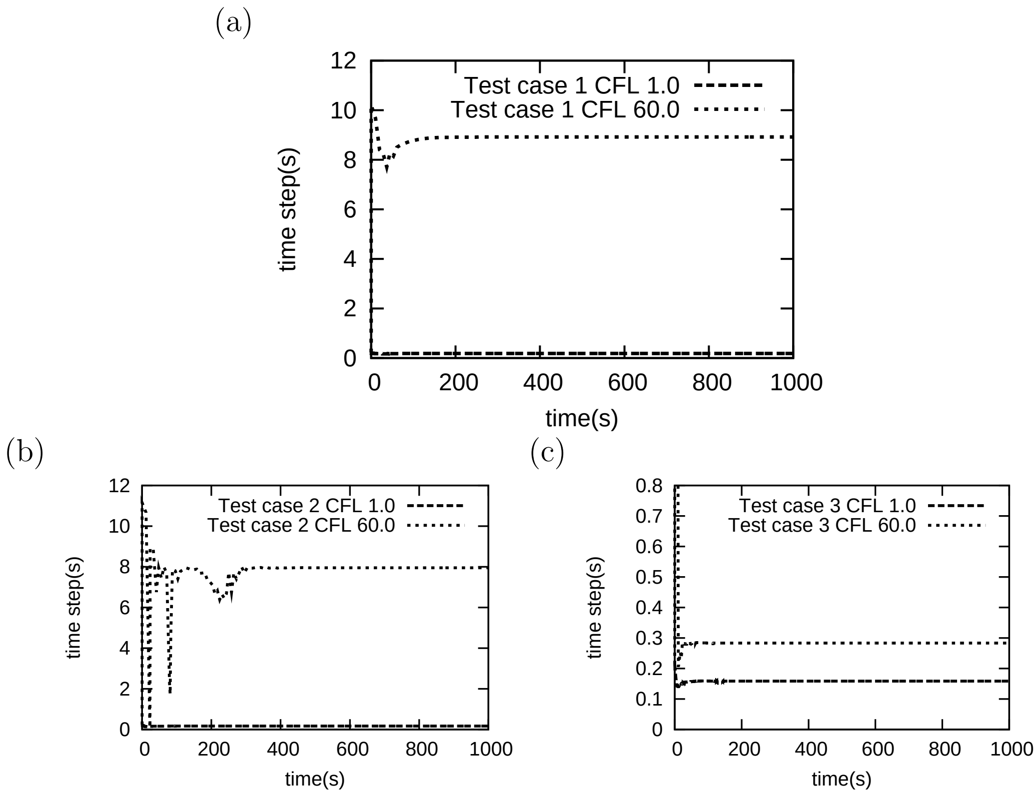

Figure 25: Evolution of the time step: (a) test case 1, (b) test case 2 and (c) test case 3

4.5.2. Application to unsteady flow: dambreak problem with source terms

The unsteady flow induced by and ideal dambreak is the most widely used test case for numerical schemes of the kind considered here. Combining it with large source terms represented by discontinuous bed becomes a powerful tool to evaluate how robust and accurate a numerical scheme can be. The results are going to be presented as follows: the numerical solution provided by the LTS scheme with CFL=5.0 ($- \bullet -$) is compared with the numerical solution obtained with the CUE scheme with CFL=1.0 ($- \circ -$) and also with the exact solution of each problem (—). The geometry of all of them is a rectangular frictionless 1 km long channel with a bottom step at $x = 0$ and a variable height at each side of the bed discontinuity. All of this test cases are included in [12] and more information about the nature and the exact solution of them can be found there.

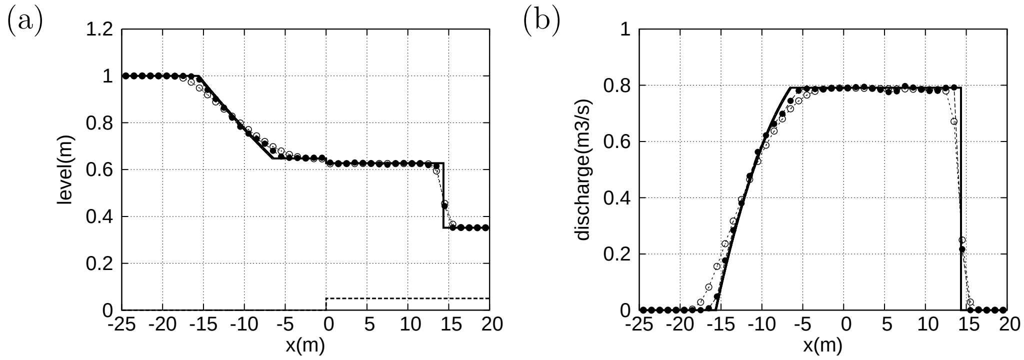

Figure 26: Test case 1: exact (—) and numerical solutions at $t = 5s$ using CFL=1.0 ($- \circ -$) and CFL=5.0 ($- \bullet -$) for (a) the water level surface, and (b) the discharge

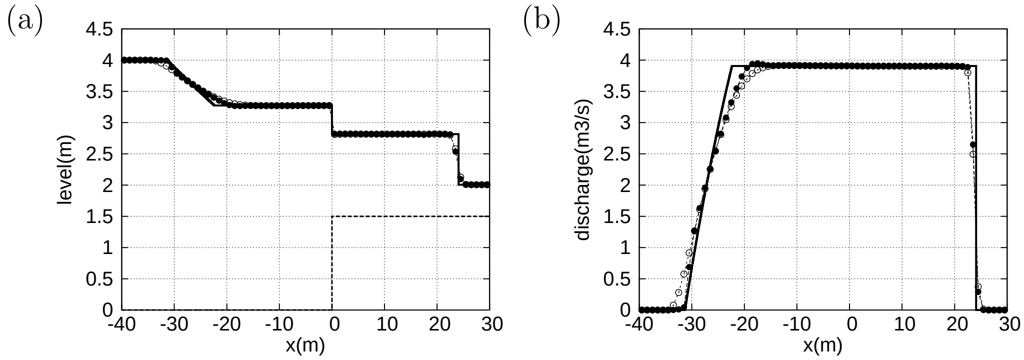

Figure 27: Test case 2: exact (—) and numerical solutions at $t = 5s$ using CFL=1.0 ($- \circ -$) and CFL=5.0 ($- \bullet -$) for (a) the water level surface, and (b) the discharge

All the test cases computed here are summarised in Table 3. The test cases chosen do not include wet/dry front since, in those cases, the LTS simply reduces to the CUE scheme.

The numerical solutions are calculated with $g = 9.8\ m^2/s$, the acceleration due to the gravity, and $\Delta x = 1.0$. Also, for the numerical solution provided by the LTS scheme, the parameter ξ in (76) using to reduce the time step at big discontinuities has been applied.

The results are presented in the form of plots of the water level surface and discharge for each test case (Figures 26–31). The topography is represented in dashed line.

Table 3: Summary of test cases.

Test Case	h_L	h_R	u_L	u_R	z_L	z_R
1	1.0	0.30179953	0.0	0.0	0.0	0.05
2	4.0	0.50537954	0.1	0.0	0.0	1.5
3	2.5	2.49977381	1.5	0.0	0.0	0.25
4	1.5	0.16664757	2.0	0.0	0.0	2.0
5	1.0	0.04112267	0.2	0.0	0.25	0.0
6	0.6	0.02599708	0.35	0.0	1.2	0.0

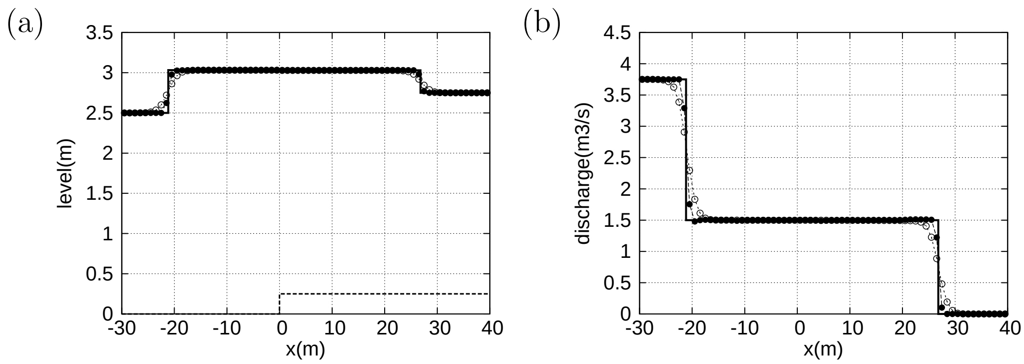

Figure 28: Test case 3: exact (—) and numerical solutions at $t = 5s$ using CFL=1.0 ($-\circ-$) and CFL=5.0 ($-\bullet-$) for (a) the water level surface, and (b) the discharge

The test cases proposed here are really extreme cases where the source term plays a leading role. Also discontinuities in the initial height and discharge make these situations in fact suitable to examine the power of a numerical method.

The results provided by the LTS scheme are as good or more accurate than those from the CUE scheme. As the time steps are larger, less of them are

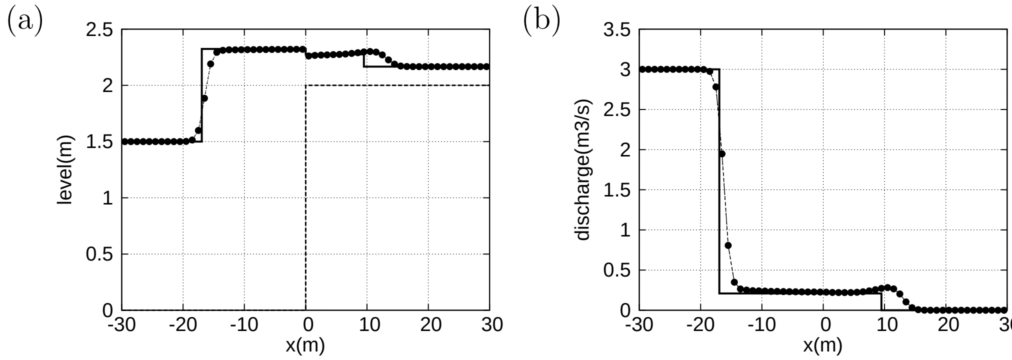

Figure 29: Test case 4: exact (—) and numerical solutions at $t = 5s$ using CFL=1.0 ($-\circ-$) and CFL=5.0 ($-\bullet-$) for (a) the water level surface, and (b) the discharge

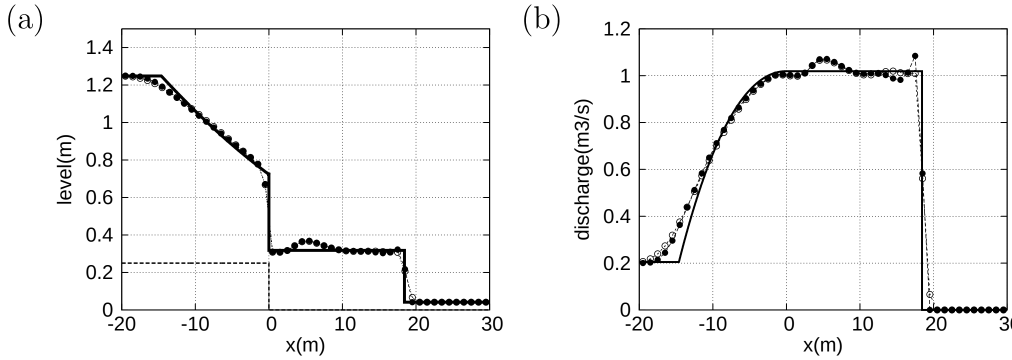

Figure 30: Test case 5: exact (—) and numerical solutions at $t = 5s$ using CFL=1.0 ($-\circ-$) and CFL=5.0 ($-\bullet-$) for (a) the water level surface, and (b) the discharge

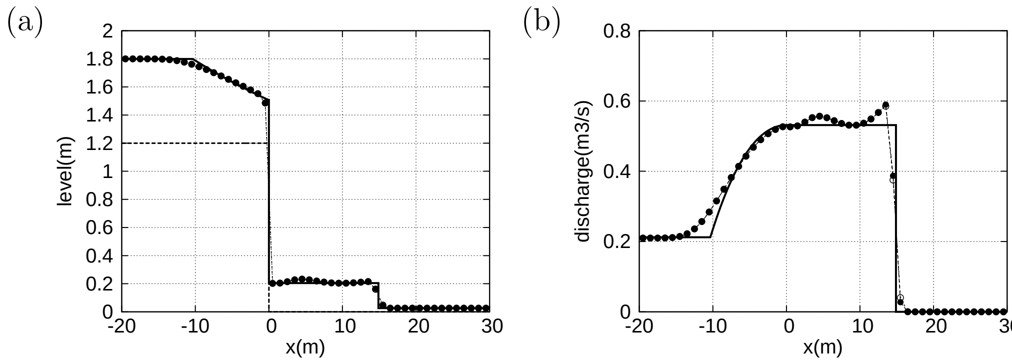

Figure 31: Test case 6: exact (—) and numerical solutions at $t = 5s$ using CFL=1.0 ($-\circ-$) and CFL=5.0 ($-\bullet-$) for (a) the water level surface, and (b) the discharge

necessary to compute the numerical solution, so it is less diffusive. Moreover, the influence of ξ is presented above all in test cases 4, 5 and 6 where this parameter is frequently less than 1 (and generally less also than 0.25). The aim of the parameter ξ is to detect when a strong discontinuity or large source term are present and to be able to generalise the LTS scheme. The examples show that in the extreme test cases, the CFL number is reduced when a large discontinuity is present. For all test cases the number of time steps necessary to compute the numerical solution is indicated in Table 4. Figure 32(a) and (b) shows also the evolution of the time step for test case 1,2,3 and 4,5,6 respectively using the LTS and CUE scheme. The shading symbols represents the conventional upwind explicit scheme and the empty symbols the LTS scheme.

Test case	**LTS scheme**	**CUE scheme**
1	5	19
2	12	34
3	8	33
4	30	30
5	19	25
6	16	20

Table 4: Time steps done by each numerical method

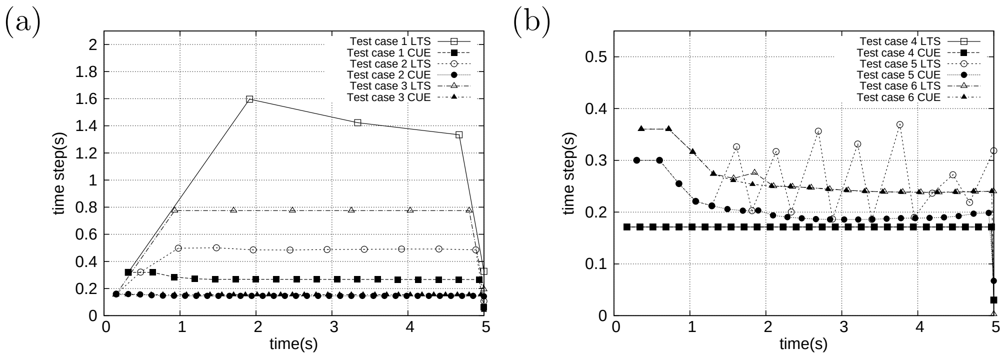

Figure 32: Evolution of the time step (a) for test cases 1, 2, 3 and (b) for test cases 4, 5, 6

5. Conclusions

In this paper, an extension of the large time step (LTS) scheme developed by Leveque has been presented in order to complete and generalise this method first for scalar equations and then for the shallow water equations with source terms.

The proposed LTS scheme, when applied to non-linear scalar cases, requires the discrete representation of the rarefaction wave in the form of several discontinuities travelling at different speeds if an accurate solution is sought at large CFL values. A simple rule to estimate these speeds has been proposed. When incorporating the presence of a source term in non-linear scalar equations, the LTS scheme can be easily extended following the same procedure as in the homogeneous case provided that the original explicit scheme was already well-balanced. However, it is important to remark that the quality of the numerical solution deteriorates as the CFL grows in presence of relatively important source terms due to the fact that the scheme is based on the advection speed of the homogeneous system. The inviscid Burgers equation with source term has been used to propose a second estimation of the advection speed that takes into account the presence of the source term in the form of an intermediate state. The effectiveness of this treatment has been illustrated for the Burgers equation with source term achieving accurate numerical solutions in a single time step.

The extension to non-linear systems of equations with source terms has been explored and applied to the 1D shallow water system. The splitting technique required in rarefactions has been extended to systems and shown to produce good results that preserve conservation. The bed slope and friction source terms have been incorporated in a compact formulation with a three wave approximate solution taking into account one extra wave associated with the source term according to previous work. From that formulation of the well-balanced explicit scheme, the extension leading to the LTS scheme has been possible. In the case of systems, the LTS shows a good performance for CFL>1 but, as in the scalar case, the solution is worse as the CFL grows in presence of strong discontinuities and/or relatively important source terms. Looking for a compromise between accuracy and efficiency in the method, instead of devising a complex procedure to improve the estimation of the advection speeds in presence of strong discontinuities and/or relatively important source terms, a new parameter ξ is proposed in order to detect these situations and to reduce accordingly the target CFL number chosen initially.

The treatment of the boundary conditions at open and closed boundaries has been explored and two possible techniques are provided for the second case. Among them, the reflection technique, that sends back the information that would cross the boundary when using large CFL values, is recommended in the case of close boundaries. At open boundaries, no special treatment is required for the information going out of the computational domain apart from the logical control of the conservation.

With the proposed modifications, the LTS scheme has been used to reproduce all kind of flow conditions. Its performance has been illustrated using test cases with exact solution of steady and unsteady open channel flow problems. In the steady open channel flow test cases, the LTS scheme has proved efficient and accurate allowing the use of very high CFL values. The technique proposed to control the size of the CFL in presence of discontinuities has been effective in the steady flow problems with hydraulic jump. A series of frictionless dam break problem with all kind of discontinuous bed level have been used as validation test cases. Again, the LTS has been supplied with the parameter dynamically controlling the appearance of strong discontinuities and/or important source terms that has been able to adjust accordingly the maximum allowable CFL value to produce accurate and stable numerical solutions.

Finally, this LTS scheme is an explicit method, and the advantages related with this kind of schemes are conserved. Moreover, the CFL condition is relaxed and larger time steps can be used, so that a computational gain and less diffusive results can be achieved in most cases. The obtained results point out that the LTS scheme is able to predict faithfully the overall behaviour of the solution and of any type of waves.

[1] E.F.Toro , Shock-Capturing Methods for Free-Surface Shallow Flows, Wiley, New York, (2001), p.109.

[2] R.J. Leveque, Large Time Step Shock-Capturing Techniques for Scalar Conservation Laws, Numerical Analysis Project, Manuscript NA-81-13 Standford Univertsity, Standford (1981).

[3] R.J. Leveque, A Large Time Step Generalization of Godunov's Method for System of Conservation Laws, SIAM J. Numer. Anal. 22, 1051–1073. (1985)

[4] A. Harten, On a large time-step high resolution scheme, Math. Comput. 46 (174) (1986) 379-399

[5] M. R. Norman, R. D. Nair and F.H.M. Semazzi, A low communication and large time step explicit finite-volume solver for non-hydrostatic atmospheric dynamics, J. Comput. Phys. 230 (2011) 1567–1584.

[6] Z. Qian and C-H. Lee, A class of large time step Godunov schemes for hyperbolic conservation laws and applications, J. Comput. Phys. 230 (2011) 7418–7440.

[7] J. Murillo, P. García-Navarro, P. Brufau, and J. Burguete, Extension of an explicit finite volume method to large time steps (CFL¿1): application to shallow water flows, International Journal of Numerical Methods in Fluids 54, (2007), 543–590.

[8] M.E. Vázquez-Cendón, Improved treatment of source terms in upwind schemes for the shallow water equations in channels with irregular geometry. Journal of Computational Physics 148, (1994), 497–498.

[9] R.J. Leveque, Finite Volume Methods for Hyperbolic Problems, Cambridge Univeristy Press, New York, (2002), p.311

[10] J. Murillo, J. Burguete, P. Brufau and P. García-Navarro, The influence of source terms on stability, accuracy and conservation in two-dimensional shallow flow simulation using triangular finite volumes, International Journal of Numerical Methods in Fluids, 54, (2007) 543–590.

[11] D.L. George, Augmented Riemann solvers for the shallow water equations over variable topography with steady states and inundation, Journal of Computational Physics, 227, (2008) 3089–3113.

[12] J. Murillo and P. García-Navarro, Weak solutions for partial differential equations with source terms: Application to the shallow water equations, J. Comput. Phys. 229 (2010) 4327–4368.

[13] E.F.Toro, Riemann solvers and numerical methods for fluid dynamics, Springer, Berlin, (1997), p.526.

[14] P.L. Roe, Approximate Riemann solvers, parameter vectors and difference schemes, Journal of Computational Physics, 43, (1981), 357–372.

[15] J. Burguete and P. García-Navarro, Efficient construction of high-resolution TVD conservative schemes for equations with source terms: application to shallow water flows, International Journal for Numerical Methods in Fluids, 37, (2001), 209–248.

[16] G. Rosatti and L.Begnudelli, The Riemann Problem for the one-dimensional, free-surface Shallow Water Equations with a bed-step: Theoretical analysis and numerical simulations, Journal of Computational Physics, 229, (2010), 760–787.

[17] I. MacDonald, M.J. Baines, N.K. Nichols and P.G. Samuels, Analytical benchmark solutions for open-channel flows, ASCE Journal of Hydraulic Engineering, 123(11), (1997), 1041-1045.

[18] I. MacDonald, Analysis and computation of steady open channel flow, PhD Thesis, University of Reading (1996)